# Spectroscopy of MXB 1658–298 in two accretion states during recent outburst

**Rahul Sharma[1*], Abdul Jaleel[1], Chetana Jain[2], Jeewan C. Pandey[3] and Anjan Dutta[1]**

[1]Department of Physics and Astrophysics, University of Delhi, Delhi
[2]Hans Raj College, University of Delhi, Delhi
[3]Aryabhatta Research Institute of Observational Sciences, Nainital, Uttarakhand

*rahul1607kumar@gmail.com

**Abstract**

MXB 1658–298 is a transient Low Mass X-ray Binary (LMXB), which shows dips, bursts and eclipses in its lightcurve. In this work, we report the broadband spectral study of this source with the *Swift*-XRT & *NuSTAR* observations made during the latest phase of enhanced X-ray emission which started in 2015. During these observations, MXB 1658–298 showed different spectral states and accretion rates. During the observation of 2015, it was in hard state (island state) while during 2016, source was in soft state (banana state). The persistent flux of 2016 observation is a factor of ∼4 larger than the 2015 observation. We will discuss and compare some interesting features observed during recent outburst of the source. We have found the connection between accretion disk atmosphere or wind and accretion state.

## Introduction

MXB 1658–298 is a Low Mass X-ray Binary (LMXB) which was discovered by SAS-3 in 1976 (Lewin et al. 1976). It shows dip, burst and eclipse behaviors. It shows periodic X-ray eclipses in every 7.1 hours, with a duration of $\sim$ 15 mins (Cominsky & Wood 1984). About 2 years after its discovery, the X-ray intensity declined and the source was not detectable for more than 20 years. After being X-ray bright for about 2.5 years since 1999, the source went into quiescence near the beginning of 2001. The 0.5-30 keV *Beppo*SAX spectrum obtained in 2000 was modeled by a combination of a soft disk blackbody and a harder Comptonised component (Oosterbroek et al. 2001). The residuals to this fit suggested the presence of emission features due to Ne-K/Fe-L and Fe-K in the spectrum. *XMM-Newton* observation in 2001 revealed the presence of narrow resonant absorption features due to O VIII, Ne X, Fe XXV and Fe XXVI, together with a broad Fe emission feature (Sidoli et al. 2001). After $\sim$ 14 years of quiescence state, source was again detected with renewed activity in August 2015 by *MAXI* observatory (Negoro et al. 2015).

Narrow absorption features from highly ionized Fe and other elements have been observed in a growing number of X-ray binaries. In particular, Fe XXV or Fe XXVI absorption lines near 7 keV were reported from several Neutron Star (NS) LMXBs (e.g., Sidoli et al. 2001; Díaz Trigo et al. 2006; Ponti et al. 2014, 2018) which were all viewed close to edge-on, many of them being dippers (Boirin et al. 2005; Díaz Trigo et al. 2006). This indicates that the highly ionized plasma probably originates in an accretion disk atmosphere or wind, which could be a common feature of accreting binaries but primarily detected in systems viewed close to edge-on (Díaz Trigo & Boirin 2013).

## Main Objectives

- Spectral study of the *Swift*-XRT and *NuSTAR* observations during the recent outburst of 2015-16.
- To investigate the variation in the spectral states and its properties between the two observations.

## Observations & Analysis

We used the X-ray observations of MXB 1658–298, carried out using *NuSTAR* and *Swift*-XRT on September 28, 2015 and April 21, 2016. We have processed *Swift*-XRT and *NuSTAR* data with HEASOFT version 6.20. We used the latest calibration files version 20170120 for *NuSTAR* and 20160609 for *Swift*-XRT. We used spectral program XSPEC version: 12.9.1 for spectral fitting. We fitted the persistent (after removing bursts, dips and eclipses) spectra extracted from *Swift*-XRT, *NuSTAR*-FPMA and *NuSTAR*-FPMB observations simultaneously. We added a constant to account for cross-calibration of different instruments. The value of constant for *NuSTAR*-FPMA was fixed to 1 and it was set free for others.

## Result & Discussion

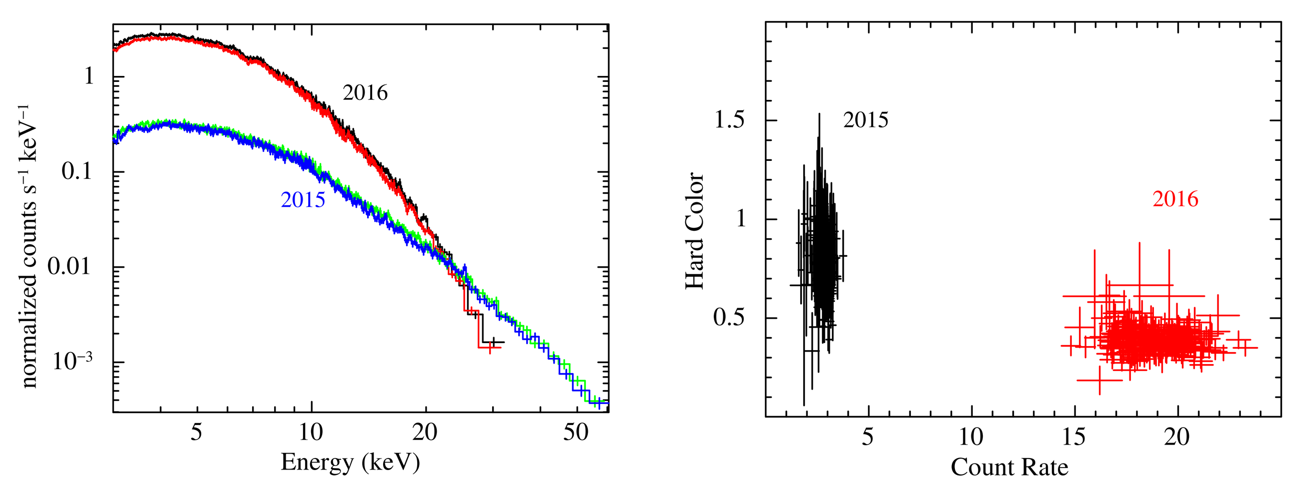


**Figure 1:** Left panel: Persistent spectrum extracted from *NuSTAR* (FPMA & FPMB) observation of 2015 and 2016. The spectrum of 2015 was hard and had low flux emission, whereas spectrum of 2016 was soft and had high flux emission. Right panel: Hardness Intensity Diagram (HID) of MXB 1658–298. The data were from FPMA only (dips, bursts and eclipses excluded). The time resolution of the data is 200 sec. The hard color is the ratio between 12–30 keV and 8–12 keV, and the count rate is in between 3–30 keV.

During the recent outburst of MXB 1658–298, source was observed at two different epochs (2015 & 2016) with *NuSTAR* and *Swift*-XRT. During these two observations, source showed two different accretion states: low hard and high soft accretion states for 2015 and 2016, respectively (see Fig. 1). During Low-Hard State (LHS) observation (2015), broadband spectrum of MXB 1658–298 can be well described with combination of two thermal (soft) component (blackbody and disk blackbody) and a hard component, thermally Comptonised continuum *compTT*. The best fit parameters are reported in Table 1. Apparent inner disk radius calculated from Norm$_{disk}$ is $15.9^{+8.5}_{-3.8}$ km, assuming inclination angle of 80° and distance of 10 kpc. We calculated the realistic inner disk radius $r_{in} = 19^{+10}_{-5}$ km by applying corrections following Kubota et al. (1998). Following in't Zand et al. (1999), we estimated the emission radius of seed photons (assuming a spherical emission) using $R_0 = 3 \times 10^4 D_{kpc}[f_{bol}/(1+y)]^{1/2}(kT_{seed})^{-2}$ km, where $D_{kpc}$ is the source distance in units of kpc, $f_{bol}$ is unabsorbed bolometric flux, $kT_{seed}$ is the seed photons temperature and $y$ is the Compton parameter defined as $y = 4kT_e\tau^2/m_ec^2$ (Relative energy gained by the photons in the inverse Compton scattering). Using best fit values with *compTT* model, we obtained Compton parameter $y = 4.4 \pm 0.7$ and emission radius of seed photons $R_0 = 10 \pm 4$ km. This implies that the soft photons are generated at the boundary layer between the accretion disk and the neutron star surface. We also estimated the electron density $n_e$ of Comptonising region from $\tau_e = n_e\sigma_T l$, where $\sigma_T$ is Thompson cross-section and $l$ is the geometrical size of of the Comptonising plasma. Assuming that the Comptonising region has a spherical geometry surrounding the NS and that it has a roughly homogeneous density and it extends up to the observed inner accretion disk radius, we found that $n_e = 5.0^{+1.2}_{-2.7} \times 10^{18} cm^{-3}$. During 2016 observation, source was in High-Soft State (HSS). Its broadband spectrum can be described with combination of blackbody and a hard component (*compTT*). It showed a systematic residuals due to absorption between 6–10 keV. These absorption residuals were modeled with an absorption line and two absorption edges (Table 1). The electron temperature of Comptonising plasma ($kT_e$) decreased to $\sim 3.6$ keV in HSS from $\sim 14.1$ keV in LHS. During LHS, Comptonising region had optical depth of 6.3 and during HSS, plasma became optical thick with optical depth of ∼9.6. This variation in electron temperature and plasma optical depth is observed during hard and soft spectral states of atoll LMXBs (Hasinger & van der Klis, 1989). We obtained Compton parameter $y = 2.6 \pm 0.2$ and emission radius of seed photons $R_0 = 4 \pm 0.5$ km for HSS. As the Comptonising region become optically thick, it will lead to higher electron density compared to LHS.

**Table 1:** Spectral parameters of MXB 1658-298 during Low-Hard State (LHS) and High-Soft state (HSS).

| Model | Parameters | LHS | HSS |
|---|---|---|---|
| TBabs | $N_H(10^{22}$ cm$^{-2})$ | $0.22^{+0.08}_{-0.07}$ | $< 0.04$ |
| diskbb | $kT_{in}$ (keV) | $0.43 \pm 0.08$ | |
| | $Norm_{disk}$ | $44^{+47}_{-21}$ | |
| bbodyrad | $kT_{bb}$ (keV) | $1.11^{+0.08}_{-0.07}$ | $0.57^{+0.02}_{-0.03}$ |
| | $Norm_{bb}$ | $0.91^{+0.25}_{-0.22}$ | $276^{+59}_{-26}$ |
| compTT | $kT_e$ (keV) | $14.1^{+1.5}_{-1.2}$ | $3.56 \pm 0.09$ |
| | $kT_{seed}$ (keV) | $= kT_{in}$ | $1.08^{+0.06}_{-0.07}$ |
| | $\tau_e$ | $6.3 \pm 0.4$ | $9.59 \pm 0.35$ |
| | $Norm(10^{-3})$ | $1.67^{+0.26}_{-0.19}$ | $33^{+2.7}_{-1.8}$ |
| | Compton parameter, $y$ | $4.4 \pm 0.7$ | $2.6 \pm 0.2$ |
| edge | $E_{edge}$ (keV) | | $7.71 \pm 0.06$ |
| | $\tau$ | | $0.15 \pm 0.02$ |
| edge | $E_{edge}$ (keV) | | $9.05 \pm 0.08$ |
| | $\tau$ | | $0.10 \pm 0.02$ |
| gauss | $E_{line}$ (keV) | | $6.77 \pm 0.03$ |
| | $\sigma$ (keV) | | $0.10^{+0.05}_{-0.09}$ |
| | Equivalent Width (eV) | | $-55 \pm 6$ |
| | Fraction$_{comp}$ | 0.92 | 0.78 |
| | †Flux$_{0.1-100\ keV}$ | $2.19 \pm 0.04$ | $8.95 \pm 0.03$ |
| | $\chi^2/dof$ | 703.5/642 | 847/839 |

Note : Fraction$_{comp}$ is the fraction of Comptonisation component in total flux. $\tau$ is the optical depth. † Unabsorbed flux in units of $10^{-10}$ erg cm$^{-2}$ s$^{-1}$. Uncertainties are given at a 90% confidence level.

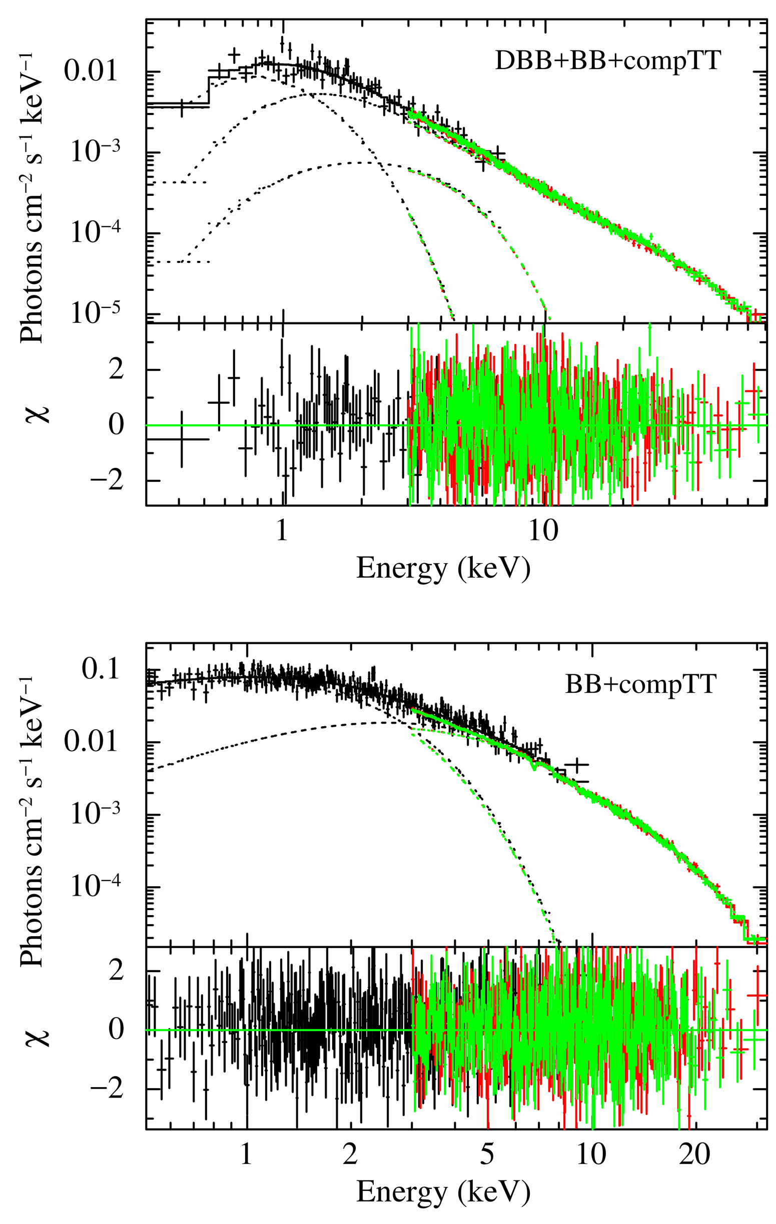


**Figure 2:** Top panel : Spectrum of 2015 observation modeled with *TBabs×(diskbb+bbodyrad+compTT)*, Bottom panel : Spectra of 2016 observation modeled with *TBabs×edge×edge×(bbodyrad+compTT+gauss)*.

The 6.77 keV absorption line is due to blend/mix of Fe XXV and Fe XXVI. The absorption edge at 9 keV is due to highly ionized Fe XXV/XXVI K edge. The 7.7 keV edge can be due to lowly ionized Fe XVI-XIX K absorption edge or Fe K emission from broad range of ionizations. We also modeled the observed absorption features with a photo-ionized absorption component *zxipcf* (assumed to be totally covering the X-ray source) instead of absorption line and edges. We note that *zxipcf* model were able to reproduce Fe K absorption lines between 6–7 keV and absorption edge at 9 keV (Fig. 3). However, the fit was not good ($\chi^2/dof = 922/844$) and residuals at 7–8 keV were still present. The column density of $\sim 10^{24}\ cm^{-2}$ and ionization parameter of $\log(\xi) \sim 4$ of ionized absorber were found from this fit. This suggests that it needs to be tested with self-consistent photo-ionization models computed on the basis of the source spectral energy distribution. The observation of intense Fe K absorption features during soft states have been found in both NS and BH systems and linked to accretion disk winds/atmosphere (e.g., Ponti et al. 2012, 2014, 2018). So, the observed absorption lines and edges in MXB 1658–298 may be due to accretion disk atmosphere or wind as the source is viewed close to edge-on. These were absent during LHS so, this suggests accretion disk atmosphere or wind and state connection. The connection between state and presence of accretion disk wind have been found in other high inclination NS LMXBs (Ponti et al. 2014, 2018).

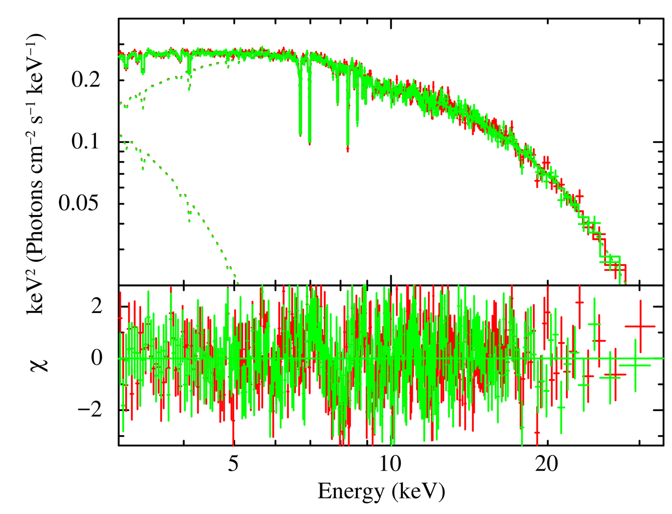


**Figure 3:** Unfolded spectra of 2016 observation, when modeled with photo-ionized absorber model *zxipcf*. For simplicity, only *NuSTAR* spectra is shown.

## Conclusions

- The spectral shape during both observations were different. The spectral parameters obtained were according to the spectral/accretion state of source.
- Electron plasma temperature ($kT_e$) decreased to 3.56 keV during HSS from 14.1 keV during LHS.
- During HSS, Comptonising plasma became optically thick ($\tau \sim 9.6$) compared to LHS ($\tau \sim 6.3$).
- Absorption line and edges were detected due to highly ionized elements (Fe XXV or Fe XXVI) in the persistent emission spectrum of 2016 observation only.
- Absorption features can be attributed to accretion disk wind or atmosphere.
- Presence of accretion disk wind or atmosphere can be linked to accretion state or disk wind and jet connection (Ponti et al. 2012).

## References

Boirin L., Méndez M., Díaz Trigo M., Parmar A. N., & Kaastra J. S., 2005, A&A, 436, 195
Cominsky L. R., & Wood K. S., 1984, ApJ, 283, 765
Díaz Trigo M., Boirin L., 2013, Acta Polytechnica, 53, 659
Díaz Trigo M., Parmar A. N., Boirin L., Méndez M., & Kaastra J. S. 2006, A&A, 445, 179
Hasinger G., van der Klis M., 1989, A&A, 225, 79
in't Zand J. J. M., et al., 1999, A&A, 345, 100
Kubota A., Tanaka Y., Makishima K., Ueda Y., Dotani T., Inoue H., Yamaoka K., 1998, PASJ, 50, 667
Lewin W. H. G., Hoffmann J. A., & Doty J., 1976, IAU Circ., 2994
Negoro H., et al., 2015, ATel, 7943, 1
Oosterbroek T., Parmar A. N., Sidoli L., in't Zand J. J. M., Heise J., 2001, A&A, 376, 532
Ponti G., Fender R. P., Begelman M. C., Dunn R. J. H., Neilsen J., Coriat M., 2012, MNRAS, 422, L11
Ponti G., Muoz-Darias T., Fender R. P., 2014, MNRAS, 444, 1829
Ponti G., et al., 2018, MNRAS, 473, 2304
Sidoli L., Oosterbroek T., Parmar A. N., Lumb D., Erd C., 2001, A&A, 379, 540